Proceeding Series of the Brazilian Society of Computational and Applied Mathematics, v. 12, n. 1, 2026.

Trabalho apresentado no XLIV CNMAC, Fundação Getulio Vargas - Rio de Janeiro - RJ, 2025.

Proceeding Series of the Brazilian Society of Computational and Applied Mathematics

Functional Error Estimates for Mimetic Difference Approximations to the Poisson Problem

Jhabriel Varela[1]
Polytechnic School – UNA / Polytechnic University Taiwan-Paraguay, Paraguay
Miguel Dumett[2]
Computational Science Research Center, San Diego State University, United States of America

Abstract. Functional a posteriori error estimates provide guaranteed upper bounds on the deviation between the exact solution and any approximation in the appropriate functional space, making them agnostic to the discretization method used to obtain the approximation. However, numerical solutions often do not belong to the correct functional space, requiring postprocessing techniques to ensure compatibility with the error estimation framework. In this article, we consider the Poisson equation as a model problem and demonstrate how to postprocess solutions obtained using mimetic differences of the Corbino-Castillo type to enable the application of functional error estimates. Numerical experiments in two dimensions confirm that the proposed postprocessing techniques yield fully computable error estimates that recover ideal convergence rates in the energy norm.

Keywords. Functional a Posteriori Error Estimates, Mimetic Differences, Interpolation Operators

1 Introduction

In the last decades, a posteriori error estimates of the functional type have been applied to a wide range of mathematical models, including linear elliptic problems, elasticity, incompressible viscous fluids and non-linear problems [6]. Since functional error estimates rely only on functional arguments of the continuous problem, they are agnostic to the numerical method used to approximate the solution. Indeed, functional error estimates are valid for *any* approximation in the same energy space as the exact weak solution.

In this work, we explore the application of functional error estimates to mimetic difference approximations to the 2D Poisson equation. In particular, we use the mimetic differences of the Corbino-Castillo type [3]. Mimetic differences of the Corbino-Castillo type provide high-order discrete analogs of fundamental differential operators while preserving key physical and geometric properties. These methods enforce local conservation principles by construction, making them particularly well-suited for modeling problems governed by conservation laws.

Unfortunately, functional error estimates cannot be directly applied to mimetic difference solutions because the primal and dual approximations do not belong to the required functional spaces. To circumvent this issue, we propose a postprocessing step [7], where the mimetic solution is interpolated to relevant nodal points using mimetic interpolants [5]. This step ensures that the postprocessed solutions are compatible with the functional error estimate framework. The rest of the article is structured as follows. In Section 2, we introduce the model problem and its weak form. In Section 3, we recall the guaranteed abstract bounds for the primal variable. Finally, in Section 4, we introduce the mimetic difference approximation and the postprocessed techniques and in Section 5 we present the numerical results.

[1]jhabriel@pol.una.py
[2]mdumett@sdsu.edu

2 The Model Problem

Let $\Omega \subset \mathbb{R}^2$ be an open, bounded domain with a smooth boundary Γ. Poisson's equation consists of finding the *potential* p such that

$$\nabla \cdot (-\nabla p) = f \ \text{ in } \ \Omega \qquad \text{and} \qquad p = 0 \ \text{ on } \ \Gamma, \tag{1}$$

where ∇ is the *nabla* operator and $f \in L^2(\Omega)$ is a source term.

Let $(\cdot,\cdot)_S$ denote the L^2 inner product over a domain S with norm $\|\cdot\|_S$. It is well known that this model admits a weak solution, which is defined as follows: Find $p \in H_0^1(\Omega)$ such that

$$(\nabla p, \nabla q)_\Omega = (f, q)_\Omega \qquad \forall\ q \in H_0^1(\Omega). \tag{2}$$

Here, $H_0^1(\Omega)$ is the usual Sobolev space of square-integrable functions with square-integrable weak gradient and zero trace on Γ. The weak form is *well-posed* under standard regularity arguments. To measure the error in the following section, we will employ the energy norm

$$|||q||| = \|\nabla q\|_\Omega \qquad \forall q \in H_0^1(\Omega). \tag{3}$$

3 Abstract Framework

In this section, we present the guaranteed upper bounds following [6]. We first present the standard result based on the global Friedrich constant and then improve it by considering a partition of the domain.

Before presenting the abstract results, we need to introduce some definitions and results from functional analysis. Recalling that $\mathbf{H}(\mathrm{div},\Omega)$ is the space of square-integrable vector-valued functions with square-integrable weak divergence, we remind that Green's theorem establishes that for any pair $(q,\mathbf{v}) \in H_0^1(\Omega) \times \mathbf{H}(\mathrm{div},\Omega)$ there holds $(\nabla\cdot\mathbf{v}, q)_\Omega + (\mathbf{v}, \nabla q)_\Omega = 0$. Recall that the Friedrich inequality states that for any $q \in H_0^1(\Omega)$, there holds $\|q\|_\Omega \le C_{\mathrm{F},\Omega}\|\nabla q\|_\Omega$, where $C_{\mathrm{F},\Omega}$ is the Friedrich constant.

Theorem 3.1 (Guaranteed upper bound on the primal variable)**.** *Let $p \in H_0^1(\Omega)$ be the solution of (2) and $q \in H_0^1(\Omega)$ arbitrary. Then, for any $\mathbf{v} \in \mathbf{H}(\mathrm{div},\Omega)$, there holds*

$$|||p - q||| \le \eta_{\mathrm{DF}}(q,\mathbf{v}) + \eta_{\mathrm{R}}(\mathbf{v}, f) =: \mathcal{M}(q,\mathbf{v},f), \tag{4}$$

where $\mathcal{M}(q,\mathbf{v},f)$ is the majorant for the deviation from the exact weak primal solution, and

$$\eta_{\mathrm{DF}}(q,\mathbf{v}) = \|\mathbf{v} + \nabla q\|_\Omega \quad \textit{and} \quad \eta_{\mathrm{R}}(\mathbf{v},f) = C_{\mathrm{F},\Omega}\|f - \nabla\cdot\mathbf{v}\|_\Omega \tag{5}$$

are respectively the diffusive error and residual error estimators.

Proof. Start by measuring the square of the difference between the exact solution $p \in H_0^1(\Omega)$ and an arbitrary potential $q \in H_0^1(\Omega)$:

$$|||p-q|||^2 = \|\nabla(p-q)\|_\Omega^2 = (\nabla(p-q), \nabla(p-q))_\Omega = (f, p-q)_\Omega + (-\nabla q, \nabla(p-q))_\Omega\,. \tag{6}$$

Here, we used (3), and the weak form (2). Let us now fix an arbitrary flux $\mathbf{v} \in \mathbf{H}(\mathrm{div},\Omega)$. Then, using Green's theorem, it holds that for the pair $(p-q,\mathbf{v}) \in H_0^1(\Omega)\times\mathbf{H}(\mathrm{div},\Omega)$, we have $-(\nabla\cdot\mathbf{v}, p-q) - (\mathbf{v}, \nabla(p-q)) = 0$. Adding this identity to (6), we get

$$|||p-q|||^2 = (f - \nabla\cdot\mathbf{v}, p-q)_\Omega + (-(\mathbf{v}+\nabla q), \nabla(p-q))_\Omega\,. \tag{7}$$

Using the Cauchy-Schwarz inequality, the Friedrich inequality, and (3), the first term of (7) can be bounded as

$$(f - \nabla \cdot \mathbf{v}, p - q)_\Omega \leq \|f - \nabla \cdot \mathbf{v}\|_\Omega \|p - q\|_\Omega \leq C_{\mathrm{F},\Omega} \|f - \nabla \cdot \mathbf{v}\|_\Omega |||p - q|||. \tag{8}$$

Using the Cauchy-Schwarz inequality and (3), the second term of (7) can be bounded as

$$(-(\mathbf{v} + \nabla q), \nabla(p - q))_\Omega \leq \|\mathbf{v} + \nabla q\|_\Omega |||p - q|||. \tag{9}$$

The proof is completed after substituting (8) and (9) in (7) and canceling common terms. □

Remark 3.1 (Nature of the estimates)**.** *The majorant $\mathcal{M}(q, \mathbf{v}, f)$ from Theorem 3.1 has two clear contributions: (i) a diffusive error that measures the difference between an arbitrary $H(div)$-flux and the flux obtained from an arbitrary H_0^1-potential, and (ii) a residual estimator that measures the difference between the exact source term and the divergence of the arbitrary $H(div)$-flux.*

In practice, the upper bound from Theorem 3.1 has the limitation that the Friedrich constant is hard to determine and often overestimates the upper bound due to its global nature. A fully computable upper bound can be obtained by considering the decomposition of the domain Ω. That is $\overline{\Omega} = \bigcup_{K \in \mathcal{T}_h} K$, where K denotes a non-overlapping subdomain of Ω and $\mathcal{T}_h$ is the set of all subdomains K. This decomposition allows us to employ the local Poincaré inequality, which states that for any $q \in H^1(K)$, $K \subset \Omega$, there holds $\|q - \{q\}_K\|_K \leq C_{\mathrm{P},K} \|\nabla q\|_K$, where $\{q\} = \frac{1}{|K|}(q, 1)_K$ is the mean value of q over K and $C_{\mathrm{P},K}$ is the local Poincaré constant. Moreover, assuming K convex, one can always bound $C_{\mathrm{P},K}$ such that $C_{\mathrm{P},K} \leq \frac{h_K}{\pi}$, where $h_K := \mathrm{diam}(K)$.

We shall require the following equivalences between global and local norms:

$$\|q\|_\Omega^2 = \sum_{K \in \mathcal{T}_h} \|q\|_K^2 \ \forall q \in L^2(\Omega) \quad \text{and} \quad |||q|||^2 = \sum_{K \in \mathcal{T}_h} \|\nabla q\|_K^2 \ \forall q \in H_0^1(\Omega). \tag{10}$$

Moreover, to ensure the validity of this new upper bound, we require the arbitrary flux $\mathbf{v} \in \mathbf{H}(\mathrm{div}, \Omega)$ entering the error estimates to conserve mass at the local level. We make this requirement explicit in the following assumption.

Assumption 3.1 (Locally mass-conservative flux)**.** *Let $\mathbf{v} \in \mathbf{H}(\mathrm{div}, \Omega)$ be fixed. Then, we say $\mathbf{v}$ is locally mass-conservative if for all $K \in \mathcal{T}_h$ satisfies $(f, 1)_K = (\nabla \cdot \mathbf{v}, 1)_K$.*

We now have all the ingredients to present the guaranteed upper bound for the primal variable in the case of local mass-conservative fluxes.

Theorem 3.2 (Guaranteed upper bound on the primal variable for local mass-conservative fluxes)**.** *Let $p \in H_0^1(\Omega)$ be the solution of (2) and $q \in H_0^1(\Omega)$ arbitrary. Then, for any function $\mathbf{v} \in \mathbf{H}(\mathrm{div}, \Omega)$ satisfying Assumption 3.1, there holds*

$$|||p - q||| \leq \eta_{\mathrm{DF}}(q, \mathbf{v}) + \eta_{\mathrm{R,LC}}(f, \mathbf{v}) =: \mathcal{M}_{\mathrm{LC}}(q, \mathbf{v}, f) \leq \mathcal{M}(q, \mathbf{v}, f), \tag{11}$$

where $\mathcal{M}_{\mathrm{LC}}(q, \boldsymbol{v}, f)$ is the majorant for the deviation from the exact weak primal solution for local mass-conservative fluxes, and

$$\eta_{\mathrm{DF}}(q, \mathbf{v}) = \left(\sum_{K \in \mathcal{T}_h} \|\mathbf{v} + \nabla q\|_K^2 \right)^{1/2} \quad \textit{and} \quad \eta_{\mathrm{R,LC}}(f, \mathbf{v}) = \left(\sum_{K \in \mathcal{T}_h} \frac{h_K^2}{\pi^2} \|f - \nabla \cdot \mathbf{v}\|_K^2 \right)^{1/2}, \tag{12}$$

are respectively the diffusive error and residual error for local mass-conservative fluxes estimators.

Proof. The proof follows the previous one, except for the first term in (7) that is now bounded as

$$\begin{aligned}(f-\nabla\cdot\mathbf{v},p-q)_\Omega &= \sum_{K\in\mathcal{T}_h}(f-\nabla\cdot\mathbf{v},p-q)_K = \sum_{K\in\mathcal{T}_h}(f-\nabla\cdot\mathbf{v},p-q-\{p-q\})_K\\ &\le \sum_{K\in\mathcal{T}_h}\|f-\nabla\cdot\mathbf{v}\|_K\|p-q-\{p-q\}\|_K \le \sum_{K\in\mathcal{T}_h}C_{\mathrm{P},K}\|f-\nabla\cdot\mathbf{v}\|_K\|\nabla(p-q)\|_K\\ &\le \sum_{K\in\mathcal{T}_h}\frac{h_K}{\pi}\|f-\nabla\cdot\mathbf{v}\|_K\|\nabla(p-q)\|_K \le \left(\sum_{K\in\mathcal{T}_h}\frac{h_K^2}{\pi^2}\|f-\nabla\cdot\mathbf{v}\|_K^2\right)^{1/2}|||p-q|||. \end{aligned}\tag{13}$$

Here, we employ the equivalence between global and broken norms, the local mass-conservative property of $\mathbf{v}$, the Cauchy-Schwarz inequality, the local Poincaré inequality, the upper bound on $C_{\mathrm{P},K}$, the Cauchy-Schwarz inequality once more, and finally the equivalence between global and broken norms. The proof is completed in a similar manner as in the previous one. □

Note that $\mathcal{M}_{\mathrm{LC}}$ is now fully computable (i.e., it does not contain undetermined constants). Moreover, since local Poincaré constants are smaller than the Friedrich constant, $\mathcal{M}_{\mathrm{LC}} \le \mathcal{M}$.

4 Mimetic Difference Approximation and Postprocessing

Mimetic differences provide discrete analogs of differential operators such as gradient ∇, divergence $\nabla\cdot$, Laplacian ∇^2, and curl $\nabla\times$. These operators are constructed to have a high-order uniform order of accuracy over the whole domain (including boundaries), to approximate the extended Gauss divergence theorem, and to mimic vector calculus identities. We will use the ones proposed by Corbino-Castillo [3]. These operators are available in the MOLE library [4].

Mimetic difference operators are defined on a *staggered grid* (see e.g., Fig. 1) where scalar and vector fields are evaluated at different locations. To write the discrete analog of equations that approximates (1), we must first introduce relevant sets. Let $\mathcal{C}$ denote the set of cell centers, $\mathcal{F}$ the set of edge centers and $\mathcal{V}$ the set of vertices. Moreover, let $\mathcal{F}_\Gamma$ denote the set of edge centers that are on the boundary of the domain, i.e., $\mathcal{F}_\Gamma := \mathcal{F}\cap\Gamma$. We will also need the set of the four nodes constituting the corners of the domain $V_{\mathrm{corner}} \subseteq V$. With the introduced sets, we define the set $\mathcal{P} := C \cup \mathcal{F}_\Gamma \cup V_{\mathrm{corner}}$. The mimetic difference method approximates the primal solution at the nodes of $\mathcal{P}$ and the dual solution at the nodes of $\mathcal{F}$. In other words, potentials are approximated at cell centers (plus some boundary nodes) whereas fluxes are approximated at edge centers. Consider now the following discrete linear operators:

$$G:\mathbb{R}^{|\mathcal{P}|}\to\mathbb{R}^{|\mathcal{F}|},\quad D:\mathbb{R}^{|\mathcal{F}|}\to\mathbb{R}^{|\mathcal{P}|},\quad L=D\circ G:\mathbb{R}^{|\mathcal{P}|}\to\mathbb{R}^{|\mathcal{P}|},\quad B=\mathbb{R}^{|\mathcal{P}|}\to\mathbb{R}^{|\mathcal{P}|}.\tag{14}$$

The first operator is the mimetic gradient G, mapping from primal to dual degrees of freedom (DoFs). The second operator is the mimetic divergence D, mapping from dual to primal DoFs. The third operator is the mimetic Laplacian L, a composed linear operator that maps from primal to primal DoFs, and B is a linear operator mapping from primal to primal DoFs handling the boundary conditions. In practice, these operators are stored as sparse matrices. Their explicit forms depend on the order of accuracy of the mimetic approximation, the grid, and the type of boundary conditions. For our purposes, an explicit representation of the operators is not necessary. The interested reader, however, is referred to [3, 4].

We shall now consider the mimetic approximation to (1). Let $\boldsymbol{p}_h = \{p_h^1,\dots,p_h^{|\mathcal{P}|}\}^T$ be the (computational) vector denoting the approximated mimetic solution and $\boldsymbol{f} = \{f^1,\dots,f^{|\mathcal{P}|}\}^T$ be the exact source term projected onto the nodes of $\mathcal{P}$. Then, the discrete linear system of equations can be written as

$$(L+B)\boldsymbol{p}_h = -\boldsymbol{f}.\tag{15}$$

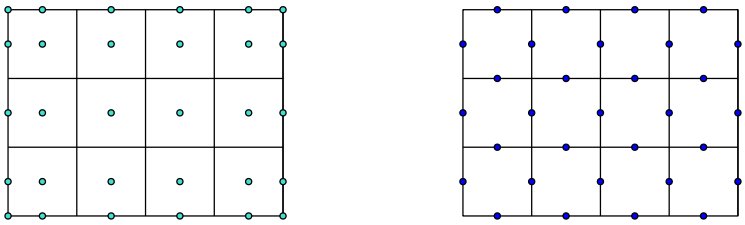

Figure 1: A 4×3 staggered grid. Left: Degrees of freedom for the primal variable (i.e., the potential). Right: Degrees of freedom for the dual variable (i.e., the flux). Source: Authors.

After solving (15), mimetic fluxes can be retrieved using $\boldsymbol{p}_h$. Let $\boldsymbol{u}_h = \{u_h^1, \ldots, u_h^{|\mathcal{F}|}\}^T$ be the approximated mimetic flux, then

$$\boldsymbol{u}_h = -G\boldsymbol{p}_h. \tag{16}$$

Recall that Theorems 3.1 and 3.2 require a potential in $H_0^1(\Omega)$ and a flux in $\mathbf{H}(\mathrm{div}, \Omega)$. However, our mimetic primal and dual solutions do not directly belong to such spaces. We must then postprocess both quantities and produce a potential $\tilde{p}_h \in H_0^1(\Omega)$ and a flux $\tilde{\mathbf{u}}_h \in \mathbf{H}(\mathrm{div}, \Omega)$. To this aim, we first introduce some relevant local finite element spaces [1].

For a rectangular element $K \subset \Omega$, we denote by $\mathbb{P}_{k_1,k_2}(K)$ the space of polynomials of degree less or equal to k_1 in x and less or equal to k_2 in y. When $k_1 = k_2$, we use $\mathbb{Q}_k(K) = \mathbb{P}_{k,k}(K)$. For the fluxes, we will need the Raviart-Thomas space of degree k, defined as $\mathbb{RT}_k(K) = \mathbb{P}_{k+1,k}(K) \times \mathbb{P}_{k,k+1}(K)$. The construction of the broken global finite element spaces is now straightforward:

$$\mathbb{Q}_k(\mathcal{T}_h) = \{q_h \in L^2(\Omega) : q_h|_K \in \mathbb{Q}_k(K) \quad \forall\, K \in \mathcal{T}_h\}, \tag{17}$$

$$\mathbb{RT}_k(\mathcal{T}_h) = \{\mathbf{v}_h \in [L^2(\Omega)]^2 : \mathbf{v}_h|_K \in \mathbb{RT}_k(K) \quad \forall\, K \in \mathcal{T}_h\}. \tag{18}$$

One can prove that $\mathbb{Q}_k(\mathcal{T}_h) \cap H_0^1(\Omega) \subset H_0^1(\Omega)$ for any $k \geq 1$, whereas $\mathbb{RT}_k(\mathcal{T}_h) \subset \mathbf{H}(\mathrm{div}, \Omega)$ for any $k \geq 0$. Thus, to obtain computable estimates [8], we need a potential $\tilde{p}_h \in \mathbb{Q}_k(\mathcal{T}_h) \cap H_0^1(\Omega)$, $k \geq 1$ and a flux $\tilde{\mathbf{u}}_h \in \mathbb{RT}_k(\mathcal{T}_h)$, $k \geq 0$. We shall fulfill the former requirement via a potential reconstruction process and the latter via extension of normal fluxes following [2, 7].

Pressure Reconstruction

Let $\boldsymbol{p}_h \in \mathbb{R}^{|\mathcal{P}|}$ be known. Moreover, let $I_{\mathcal{P}\to\mathcal{V}} : \mathbb{R}^{|\mathcal{P}|} \to \mathbb{R}^{|\mathcal{V}|}$ be the mimetic interpolant from primal DoFs to vertices, and let $I_{\mathcal{P}\to\mathcal{F}} : \mathbb{R}^{|\mathcal{P}|} \to \mathbb{R}^{|\mathcal{F}|}$ be the mimetic interpolant from primal DoFs to edge centers. Then, construct the set of Lagrangian nodes $\mathcal{L}_2 = \{\boldsymbol{p}_h, I_{\mathcal{P}\to\mathcal{V}}\boldsymbol{p}_h, I_{\mathcal{P}\to\mathcal{F}}\boldsymbol{p}_h\}$, and from there obtain:

$$\tilde{p}_h|_K = \sum_{i=1}^{9} \pi_i \phi_i \in \mathbb{Q}_2(K), \quad \forall K \in \mathcal{T}_h, \tag{19}$$

where $\pi_i \in \mathcal{L}_2$ and ϕ_i is the standard Lagrange basis function. With each $\tilde{p}_h|_K \in \mathbb{Q}_2(K)$, we can now construct the global piecewise quadratic function $\tilde{p}_h \in \mathbb{Q}_2(\mathcal{T}_h)$.

Flux Extension

Let $\boldsymbol{u}_h \in \mathbb{R}^{|\mathcal{F}|}$ be known. Then, extend the edge fluxes into each element using Raviart-Thomas basis functions [2]:

$$\tilde{\mathbf{u}}_h|_K = \sum_{j=1}^{4} u_{h,j} \boldsymbol{\psi}_j \ \in \mathbb{RT}_0(K), \quad \forall K \in \mathcal{T}_h, \tag{20}$$

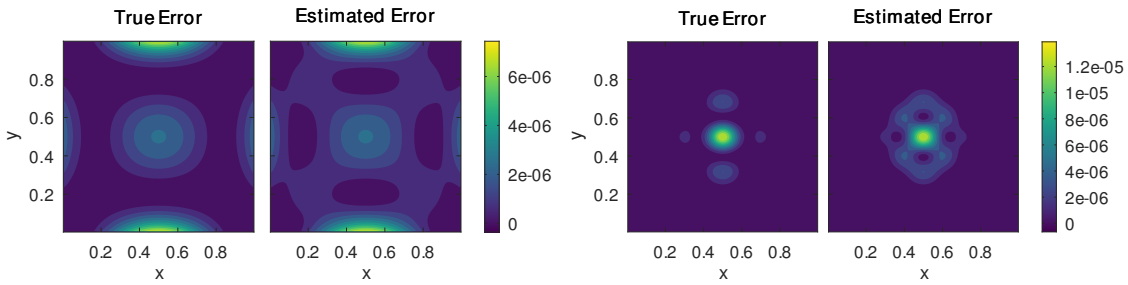

Figure 2: True and estimated error fields. Left: Quartic field. Right: Symmetric oscillatory Gaussian field. Source: Authors.

where $\boldsymbol{\psi}_j$ are the lowest-order Raviart-Thomas basis functions on each edge and $u_{h,j}$ are the known flux values at the edge centers. With each $\tilde{\mathbf{u}}_h|_K \in \mathbb{RT}_0(K)$, we can now construct $\tilde{\mathbf{u}}_h \in \mathbb{RT}_0(\mathcal{T}_h)$. Notably, the extended flux $\tilde{\mathbf{u}}_h$ satisfies the divergence constraint in each element $K \in \mathcal{T}_h$, ensuring local conservation.

Having available the post-processed pair $(\tilde{p}_h, \tilde{\mathbf{u}}_h)$, fully computable error estimates are immediate by setting $(q, \mathbf{v}) = (\tilde{p}_h, \tilde{\mathbf{u}}_h)$ in Theorem 3.2.

5 Numerical Tests

In this section, we assess the efficiency of our error estimates by applying them to two different manufactured solutions. Both examples employed mimetic approximations of second order and the domain is the unit square. Numerical examples are available at `www.github.com/jhabriel/mimetic_a_posteriori.git`. To quantify the efficacy of our estimates, we introduce the efficiency index $I_{\text{eff}} := \mathcal{M}_{\text{LC}}(\tilde{p}_h, \tilde{\mathbf{u}}_h, f)/|||p - \tilde{p}_h|||$. Note that according to Theorem 3.2, $I_{\text{eff}} \geq 1$ and $I_{\text{eff}} = 1$ only when $(\tilde{q}_h, \tilde{\mathbf{u}}_h) = (p, -\nabla p)$.

In the first numerical test, we consider an exact potential field given by the quartic polynomial $p(x, y) = 1000x^2(1-x)^2y(1-y)^2$, whereas in the second example we employ a symmetric oscillatory Gaussian potential field given by $p(x, y) = e^{-\alpha((x-0.5)^2+(y-0.5)^2)} \cos(\beta(x - 0.5)) \cos(\beta(y - 0.5))$, where α controls the Gaussian steepness and β the frequency of the cosine wave—we adopt $\alpha = 20$ and $\beta = 10$ which provides a decent balance between complexity and smoothness.

The analysis is carried out for five levels of refinement using $\Delta x = \Delta y \in \{\frac{0.1}{2^n}\}_{n=0}^{4}$. Figure 2 shows the contours of the true errors and the estimated errors for the finest grid resolution. In both cases, we can see that the error estimators effectively capture the zones of larger errors. Figure 3 shows the convergence rates and the efficiency indices as a function of the number of grid cells. There are two important points to remark: (i) The majorant $\mathcal{M}_{\text{LC}}$ decreases at the same (linear) rate as the true error $|||p - \tilde{p}_h|||$, and (ii) $I_{\text{eff}} \to 1$ as the number of cells increases.

In conclusion, we have successfully obtained guaranteed and fully computable error estimates for mimetic differences of the Corbino-Castillo type. Importantly, error fields such as those from Fig. 2 can be used to effectively guide adaptive mesh refinement/coarsening strategies.

Acknowledgment

J. V. was funded by the Paraguayan National Council of Science and Technology (CONACYT) through the program Advanced Human Capital Insertion in Academia PRIA01-8.

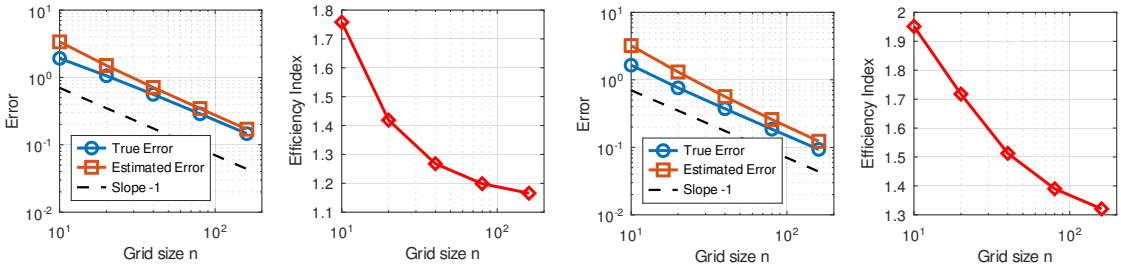

Figure 3: Convergence rates and efficiency indices. Left: Quartic field. Right: Symmetric oscillatory Gaussian field. Source: Authors.

References

[1] D. Boffi, F. Brezzi, and M. Fortin. **Mixed finite element methods and applications**. Vol. 44. Springer, 2013.

[2] S. Cochez-Dhondt, S. Nicaise, and S. Repin. "A posteriori error estimates for finite volume approximations". In: **Mathematical Modelling of Natural Phenomena** 4.1 (2009), pp. 106–122.

[3] J. Corbino and J. E. Castillo. "High-order mimetic finite-difference operators satisfying the extended Gauss divergence theorem". In: **Journal of Computational and Applied Mathematics** 364 (2020), p. 112326.

[4] J. Corbino, M. A. Dumett, and J. E. Castillo. "MOLE: Mimetic Operators Library Enhanced". In: **Journal of Open Source Software** 9.99 (2024), p. 6288.

[5] M. A. Dumett. **High-Order interpolants for derivatives of smooth functions restricted to hexahedral nodes**. Tech. rep. CSRCR2024-09. Computational Science Research Center, San Diego State University, Dec. 2024.

[6] S. Repin. **A posteriori estimates for partial differential equations**. de Gruyter, 2008.

[7] J. Varela and M. A. Dumett. **Postprocessing of Corbino-Castillo mimetic difference solutions for error estimation**. Tech. rep. CSRCR2025-03. Computational Science Research Center, San Diego State University, May 2025.

[8] M. Vohralík. **A posteriori numerical analysis based on the method of equilibrated fluxes**. Lecture Notes of Course NMNV464, Faculty of Mathemtaics and Physics, Charles Univeristy, Prague. 2024.

